

# Dichroic mirror embedded in a submicrometer waveguide for enhanced resonant nonlinear optical devices

Luigi Scaccabarozzi and M. M. Fejer

*Department of Applied Physics, Stanford University, Stanford, California 94305*

Yijie Huo and Shanhui Fan

*Department of Electrical Engineering, Stanford University, Stanford, California 94305*

Xiaojun Yu and James S. Harris

*Department of Materials Science, Stanford University, Stanford, California 94305*

Received June 26, 2006; accepted August 4, 2006;

posted August 30, 2006 (Doc. ID 72348); published October 26, 2006

We report the design, fabrication and characterization of novel dichroic mirrors embedded in a tightly confining AlGaAs/Al<sub>x</sub>O<sub>y</sub> waveguide. Reflection at the first-harmonic wavelength as high as 93% is achieved, while high transmission is maintained at the second-harmonic wavelength. The measured cavity spectrum is in excellent agreement with finite-difference time-domain simulations. Such a mirror is essential for achieving resonant enhancement of second-harmonic generation. © 2006 Optical Society of America

*OCIS codes:* 130.3120, 190.4360, 230.7370, 230.4040.

Recently there has been great interest in developing GaAs for nonlinear optics applications, such as wavelength conversion.<sup>1–3</sup> GaAs has a  $\chi^{(2)}$  coefficient that is five times larger than that of a conventional nonlinear optical material<sup>4</sup> such as LiNbO<sub>3</sub> and can be processed by well-established nanofabrication technology. Moreover, passive and active devices could be integrated on the same substrate, which is important for the realization of photonic circuits on a chip.

Until now, all nonlinear optical waveguide devices in GaAs have required at least millimeter-long interaction lengths to achieve significant conversion efficiencies.<sup>5–7</sup> In this Letter we report a demonstration of a dichroic mirror, which is an essential component for miniaturization of nonlinear optical components in GaAs.

A standard way to enhance nonlinear optical effects and to reduce the interaction length is to use a resonant cavity. For second-harmonic generation, resonating the first harmonic (FH) without resonating the second harmonic (SH) results in an enhancement ratio proportional to  $F_1^2$  and a structure tolerant to fabrication error. ( $F_1$  is the finesse of the cavity at the FH). To do this, one needs to provide a dichroic mirror that is highly reflective at the FH and transmissive at the SH. However, as we show below, in a waveguide without proper design, the SH can be strongly scattered by the mirror, resulting in significant SH loss.

In this paper we present a novel integrated dichroic mirror that is highly reflective at 1.55  $\mu\text{m}$  over a wavelength range of more than 40 nm, enough to cover the C band in telecommunication applications. Moreover, it efficiently transmits the SH around 775 nm. The fabrication of this mirror does not involve any additional processing steps beyond what is

required to fabricate a simple waveguide. This mirror should permit the realization of ultracompact ( $\sim 100 \mu\text{m}$  long) cavity devices that can be used for wavelength conversion.<sup>8</sup>

We demonstrate this mirror for birefringently phase-matched, tightly confining AlGaAs/(Al<sub>x</sub>O<sub>y</sub>) waveguides.<sup>9,10</sup> These single-mode waveguides consist of an Al<sub>0.5</sub>Ga<sub>0.5</sub>As/Al<sub>x</sub>O<sub>y</sub>/Al<sub>0.5</sub>Ga<sub>0.5</sub>As multilayer core on top of an Al<sub>x</sub>O<sub>y</sub> cladding. Dry etching provides lateral confinement. The total core size is  $\sim 300 \text{ nm} \times 900 \text{ nm}$ . The TE FH mode is phase matched to the TM SH mode.

The typical way to create a reflector for such a waveguide is to etch a periodic grating in the top or in the sidewalls of the waveguide.<sup>11</sup> However, as is shown in Fig. 1(a), the SH transmission is strongly suppressed. The mechanism for the suppression of the SH transmission can be understood by analyzing the band diagram<sup>12</sup> of such system schematically, shown in Fig. 1(b). A periodic modulation of period  $a = \lambda_{\omega_0}/2$  opens a bandgap at the FH frequency  $\omega_0$ . The same periodicity, however, results in the SH's ( $2\omega_0$ ) being completely confined above the light line, where only radiation modes exist. Consequently, most conventional distributed Bragg reflectors created for reflecting at the FH possess poor SH transmission efficiency.

Figure 1(c) shows the design of our dichroic mirror and the simulated optical characteristics, where we see that the SH transmission remains above 90%. Taking advantage of the difference in mode size between the TE FH mode and the significantly smaller SH TM mode, we place the index modulation outside of the waveguide. In this way the SH does not see the mirror and is transmitted undisturbed. To further enhance this effect, the waveguide is tapered from the

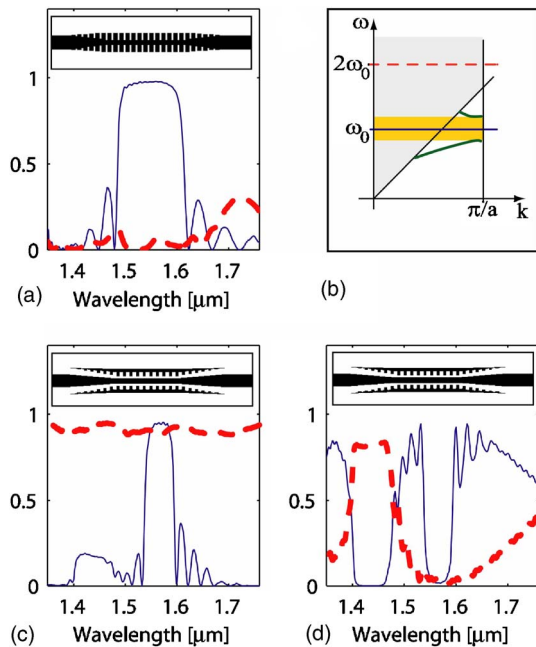


Fig. 1. (Color online) (a) Reflection (thin blue curve) at the FH wavelength and transmission (thick red curve) at the SH wavelength for a typical DBR mirror. (b) Schematic of band diagram for a distributed Bragg reflector mirror in a waveguide. The FH ( $\omega_0$ ) and SH ( $2\omega_0$ ) frequencies are shown. The shaded area is the radiation modes region. (c) FH reflection (thin blue) and SH transmission (thick red) for a 30-pair external mirror design. (d) FH transmission (thin blue) and loss (thick red) for our mirror.

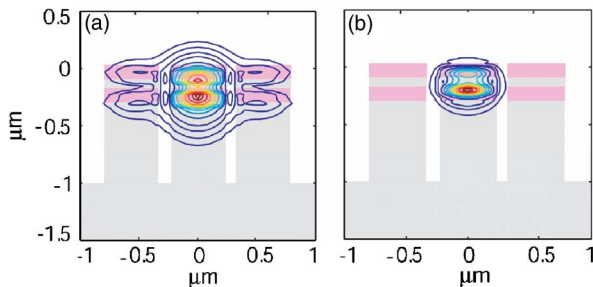


Fig. 2. (Color online) Intensity profile of (a) TE FH and (b) TM SH inside the mirror tooth. The light gray regions are  $\text{Al}_x\text{O}_y$ ; the darker (pink) regions are AlGaAs.

phase-matching width of 800–1000 nm down to 480 nm. The larger FH mode can then strongly interact with the mirror teeth, whereas the smaller TM SH mode is not significantly affected, as shown by the finite-difference time-domain (FDTD) simulation of Fig. 2. The external connection between the teeth allows the continuity of the electric field lines inside the mirror, which is essential for the high FH reflectivity. The tapered mirror shape is also essential to achieving low coupling loss (less than 5%) between the cavity and the mirror [Fig. 1(d)].

The fabrication process starts with the growth of the waveguide structure by molecular beam epitaxy. Electron-beam lithography is employed on an 80 nm thick layer of poly (methylmethacrylate) (PMMA) to define the waveguide and mirror pattern. A 20 nm chromium layer is evaporated, and the pattern is transferred into the hard chromium mask by liftoff.

The sample is then dry etched in a reactive-ion-etching–electron-cyclotron-resonance reactor in chlorine-based plasma. The remaining chromium is removed in oxygen plasma at high temperature. Then the cladding is oxidized in a water-vapor-saturated nitrogen atmosphere at 425°C. Figure 3 shows the device at the end of the fabrication process. This process gives exceptionally smooth sidewalls, with a peak-to-peak roughness of ~6 nm in the waveguide region and 8–10 nm in the mirror region.

The mirror has been characterized at both the FH and the SH wavelengths. Figure 4(a) shows the transmission of an 80 μm long cavity realized by using a 20-pair mirror with a 20-pair mirror taper on each side. The modulation period is 500 nm, which

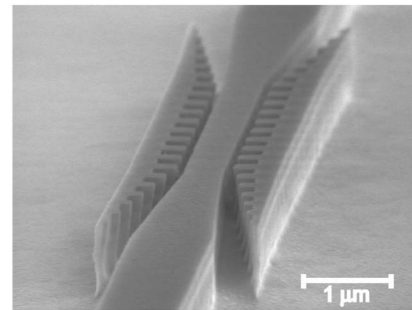


Fig. 3. SEM micrograph of the mirror at the end of the fabrication process.

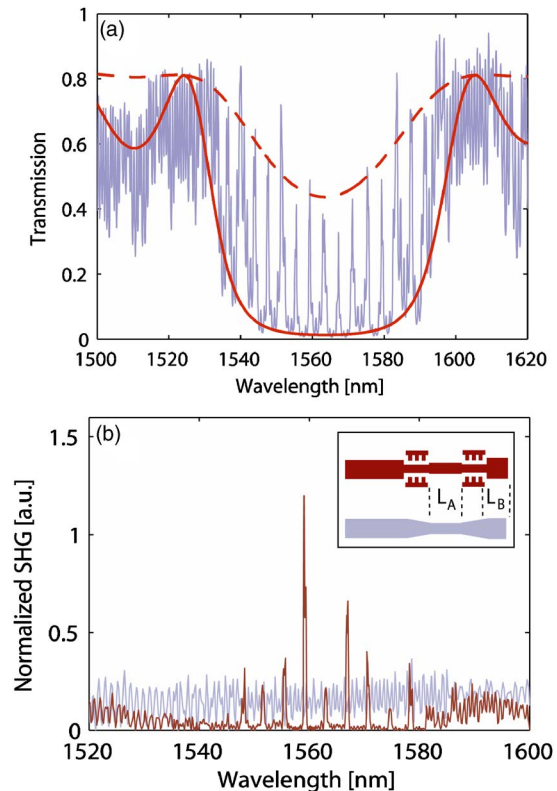


Fig. 4. (Color online) (a) Example of experimental (solid gray or blue curve) and fitted maximum (dashed black or red curve) and minimum (solid black or red curve) transmission spectra of a cavity. Fitting of fringes and cavity modes are not displayed for clarity. (b) Example of SH generated by a cavity (black or red) and by a plain waveguide of the same length (gray or blue).

gives a center gap wavelength of 1565 nm. The depth of the tooth is 280 nm; the connector is 200 nm wide. The distance between the waveguide and the teeth is 120 nm. To determine the transmission of the mirrors in the presence of the spurious Fabry–Perot fringes due to the input and output waveguide facets, we simulate the entire device (including cavity and facets) by using a 1D nonlinear transfer function algorithm.<sup>13</sup> The model was then fitted to the experimental spectrum. The fitted transmission, where, for clarity, we artificially suppress fringes and cavity modes (which also are in good agreement with the data), is also plotted in Fig. 4(a).

From the fitting, we can easily extract the parameters relative to the single mirror and compare them with the FDTD simulation. The maximum reflectivity for 20 pairs is  $\sim 75\%$ , and the loss is  $\sim 4\%$ , in very good agreement with the expected values. Although a reflectivity as high as  $\sim 95\%$  is achievable with longer mirrors, a 20-pair mirror is easier to characterize and achieves higher efficiency under the current propagation loss conditions.

Measuring the transmission at the SH is more difficult, since at this wavelength the waveguide is multimode and the propagation loss is high (estimated 25–35 dB/mm). We estimate the transmission loss of the SH by measuring the power of the SH generated by a cavity and comparing it with the SH generated from a section of plain waveguide of the same length as the cavity [Fig. 4(b)]. For the cavity, the normalized conversion efficiency can be expressed as

$$P_{2\omega\text{-out}}/P_{\omega\text{-in}}^2|_{\text{cav}} = P_{\text{SP}}\Gamma_{\omega}T_{2\omega}\exp(-\alpha_{2\omega}L_B),$$

where  $P_{\text{SP}}$  is the single-pass SH power generated in the cavity length  $L_A$ ,  $\Gamma_{\omega}$  the enhancement due to the cavity,  $T_{2\omega}$  the SH mirror transmission,  $\alpha_{2\omega}$  the SH propagation loss, and  $L_B$  the length of the last section of different width (i.e., non-phase-matched). Using the same notation, the efficiency of the plain waveguide is then written simply as

$$P_{2\omega\text{-out}}/P_{\omega\text{-in}}^2|_{\text{wg}} = P_{\text{SP}}\exp(-\alpha_{2\omega}L_B).$$

We see that the ratio of cavity efficiency to the waveguide efficiency (obtained from the experiment) does not depend on the SHG efficiency or the propagation loss. Using the enhancement ratio  $\Gamma_{\omega}$  of 6.2–6.5 estimated from the fitting of the FH spectrum, we can then estimate the SH transmission and verify the consistency of the result with the nonlinear

transfer function algorithm mentioned above. Further details about SH generation and enhancement have been reported separately.<sup>8</sup>

In conclusion, we have designed, fabricated, and characterized dichroic mirrors embedded in a tightly confining AlGaAs/Al<sub>x</sub>O<sub>y</sub> waveguide. We showed that this mirror can be used to enhance nonlinear optical effects and could lead toward the fabrication of ultra-compact nonlinear optical devices.

We acknowledge M. L. Povinelli for her help with the FDTD simulations and Charles and Evans Associates for material analysis. This research was supported by the U.S. Air Force Office of Scientific Research under grant F49620-01-1-0428. Y. Huo's e-mail address is yjhuo@stanford.edu.

## References

1. P. P. Absil, J. V. Hryniewicz, B. E. Little, P. S. Cho, R. A. Wilson, L. G. Joneckis, and P. T. Ho, *Opt. Lett.* **25**, 554 (2000).
2. T. Kondo and I. Shoji, in *Photonics Based on Wavelength Integration and Manipulation*, IPAP Books 2, K. Tada, T. Suhara, K. Kikuchi, K. Kokubun, K. Utaka, M. Asada, F. Koyama, and T. Arakawa, eds. (Institute of Pure and Applied Physics, 2005), p. 151.
3. D. Artigas, E. U. Rafailov, P. Loza-Alvarez, and W. Sibbett, *IEEE J. Quantum Electron.* **40**, 1122 (2004).
4. T. Skauli, K. L. Vodopyanov, T. J. Pinguet, A. Schober, O. Levi, L. A. Eyres, M. M. Fejer, J. S. Harris, B. Gerard, L. Becouarn, E. Lallier, and G. Arisholm, *Opt. Lett.* **27**, 628 (2002).
5. X. Yu, L. Scaccabarozzi, J. S. Harris, P. S. Kuo, and M. M. Fejer, *Opt. Express* **13**, 10742 (2005).
6. A. Fiore, S. Janz, L. Delobel, P. van der Meer, P. Bravetti, V. Berger, E. Rosencher, and J. Nagle, *Appl. Phys. Lett.* **72**, 2942 (1998).
7. S. J. B. Yoo, C. Caneau, R. Bhat, M. A. Koza, A. Rajhel, and N. Antoniadis, *Appl. Phys. Lett.* **68**, 2609 (1996).
8. L. Scaccabarozzi, Y. Huo, X. Yu, S. Fan, M. M. Fejer, and J. S. Harris, *Opt. Lett.* (to be published).
9. S. V. Rao, K. Moutzouris, and M. Ebrahimzadeh, *J. Opt. A, Pure Appl. Opt.* **6**, 569 (2004).
10. L. Scaccabarozzi, X. Yu, M. L. Povinelli, S. Fan, M. M. Fejer, and J. S. Harris, in *Proceedings of Conference on Lasers and Electro-optics*, postdeadline session (Optical Society of America, 2005), paper CPDA10.
11. P. V. Studenkov, F. Xia, M. R. Gokhale, and S. R. Forrest, *IEEE Photon. Technol. Lett.* **12**, 468 (2000).
12. S. G. Johnson, S. Fan, P. R. Villeneuve, J. D. Joannopoulos, and L. A. Kolodziejski, *Phys. Rev. B* **60**, 5751 (1999).
13. D. S. Bethune, *J. Opt. Soc. Am. B* **6**, 910 (1989).